Results in Engineering 17 (2023) 100870

Contents lists available at ScienceDirect

Results in Engineering

journal homepage: www.sciencedirect.com/journal/results-in-engineering

Solving the capacitor placement problem in radial distribution networks

Menna Allah El-sayed Mohamed El-Saeed [a,*], Amal Farouk Abdel-Gwaad [b], Mohamed AbdEl-fattah Farahat [a]

[a] Department of Electrical Power and Machines Engineering, Zagazig University, Zagazig, 44519, Egypt
[b] Faculty of Computers and Informatics, Zagazig University, Zagazig, 44519, Egypt

ARTICLE INFO

Keywords:
Capacitor placement
Distribution networks
Fuzzy logic
NSGA-II
Pareto optimization

ABSTRACT

The optimal capacitor allocation problem is suggested in this article. This study purposes to maximize the voltage stability, minimize the power losses, and consolidate the annual net savings. Calculating the optimal locations and sizes of fixed and switched capacitors is done in two steps. The first step is using the fuzzy expert rules in calculating the most candidate buses for capacitor allocation. While the second step is using a nondominated sorting genetic algorithm II (NSGA-II) in determining the list of Pareto optimal solutions and then applying a fuzzy decision maker to pick the most compromise. To emphasize the effectiveness of the proposed method, radial distribution systems are proposed; IEEE 33-bus system and the actual Portuguese IEEE 94-bus system. To demonstrate the strength and applicability of this method, a multiobjective water cycle algorithm (MOWCA), multiobjective grey wolf optimizer (MOGWO), and other optimizers used in the published papers are used. From simulation and analysis, the proposed NSGA-II outperforms other optimizers considered for comparison in achieving the maximum percentages of minimization in a real power loss of 32.369% and 31.1011% for the 33-bus system and 25.6296% and 25.3027% for the 94-bus system, the maximum percentages of minimization in a reactive power loss of 31.7916% and 30.4948% for 33-bus system and 25.9457% and 25.8001% for the 94-bus system, the maximum annual net savings of 23,612 $ and 23,131 $ for the 33-bus system for fixed and switched capacitors, respectively, and boosting the total voltage stability, which show its superior ability to give high-grade solutions.

1. Introduction

The problem of improving the performance of distribution systems has received a lot of attention from researchers and distribution system operators. Control elements can be utilized for voltage control and reactive power support such as voltage regulators and switched capacitors at substation and feeder and load tap changing (LTC) at substation transformers [1]. The installation of capacitors into the distribution network compensates the electrical loss in the distribution systems, which is about 13% of the energy generated. These high losses are caused by the need for reactive power support at the distribution level. Moreover, these losses have a negative impact on the voltage profile. It has been widely conceded that the correct position and rating of shunt capacitors in radial distribution networks (RDNs) would lead to get economic benefits such as minimizing peak power loss and energy loss against the capacitor costs while promoting the voltage profile within desired limits [2]. Fixed capacitors are operated all the time, while switched capacitors are operated depending on load levels. These capacitors are switched according to some control parameters such as voltage, current, temperature, time, and reactive power. The disadvantage of using switched capacitors is the transient overvoltages. When the industrial loads exist in the distribution feeders, capacitors are repeatedly switched on time in the expectation of an increased load at the beginning of the working day [3]. Switched capacitors also cause some drawbacks such as adjustable speed-drive trips and malfunctions of other electronically controlled load equipment [3,4].

Over the years, several approaches depending on both classical mathematical approaches and more recent metaheuristics techniques have been intensely proposed in many published papers for research in this scope. Evolving techniques such as fuzzy logic [5,6], genetic algorithms (GA), artificial neural networks, and simulated annealing [5] have been described for locating and sizing capacitors on an individual feeder. An approach based on the 2/3 rule is utilized in Ref. [7] to determine the optimal capacitor placement (OCP) on feeders

* Corresponding author.
E-mail address: m.gouda021@eng.zu.edu.eg (M.A.E.-s. Mohamed El-Saeed).

https://doi.org/10.1016/j.rineng.2022.100870
Received 26 October 2022; Received in revised form 9 December 2022; Accepted 27 December 2022
Available online 28 December 2022

considering uniformly distributed loads and randomly distributed variable spot loads. The particle swarm optimization (PSO) approach is outlined for OCP [8] with Gaussian and Cauchy probability distributions to create random values for modifying velocity [8,9]. Algorithms have been applied for calculating the optimum rating and location of capacitors for improving voltage stability [10,11]; optimizing the system to maximize voltage stability along with loss reduction has been investigated in Refs. [12–14]. The optimal allocation of shunt capacitors is addressed in three-phase distribution systems for minimizing loss and harmonic distortion under nonlinear and unbalanced loads [15]. A genetic algorithm-based method is suggested in Ref. [16] for allocating the capacitors in radial distribution systems accounting for uncertainty and time-varying loads. A voltage-dependent approach is applied to solve the OCP on distribution primary feeders [17]. A dynamic data structure with a fuzzy evolutionary programming algorithm are proposed to solve OCP considering the current reactive-power sources, transformer taps, and reconfiguration choices under different levels of loading and time intervals [18]. The problem has been developed in Refs. [19,20] to select the best position and rating of capacitors using an analytical method. A fuzzy-based methodology for multiobjective network reconfiguration and capacitor allocation in balanced and unbalanced RDNs using a hybrid big bang–big crunch algorithm is suggested in Ref. [21]. In Ref. [22], the capacitor placement problem is discussed to minimize system costs and boost annual net savings in radial test distribution networks; 10-bus, 69-bus, and 118-bus systems. The possible locations for capacitor placement are calculated using two parameters; loss sensitivity factors and the voltage stability index. A flower pollination algorithm is applied to determine the optimal locations and sizes of capacitors. From the combined results, the proposed method has proven the effectiveness in reducing losses and enhancing total savings and voltage profile in radial distribution systems under various loading conditions. In Ref. [23], a hybrid grey wolf optimizer is proposed to solve the optimal capacitor allocation problem in radial distribution systems. The hybrid grey wolf optimizer (HGWO) is a grey wolf optimizer (GWO) hybridized with mutation and crossover. The purpose is a reduction of power loss and capacitor installation costs. The proposed approach is applied in IEEE 34-, 69-, 119 bus RDNs and a practical 22-bus RDN. Comparisons with the methods mentioned in the literature have shown the power of this method and that it is a suitable optimizing tool for solving the problem of optimal capacitor allocation. In Ref. [24], a modified honey bee mating optimization algorithm (HBMO) is used to solve the optimal capacitor placement problem in primary distribution feeders considering constant and varying load conditions. Improvement of voltage profile and reduction of power losses are the objectives of this study. Comparisons with other optimizer found in the literature have revealed that this method achieves high performance and effectiveness in solving the optimal capacitor placement problem.

Multiobjective optimization problems generally consist of conflicting purposes requiring simultaneous optimization. Many real engineering problems, or even most of them, basically deal with multiple objectives, i.e. reduce cost, improve stability, consolidate reliability, etc [25]. The Pareto-front approach is the best way to solve the multivector objectives by finding a set of trade-off solutions, known as nondominated solutions or Pareto optimality of solutions. Moreover, nondominated solutions are preserved in an archive improved every iteration [26], and then the best compromise is chosen according to good provisions between them [27]. Many intelligent multiobjective algorithms are implemented in the published papers with various levels of formulations e.g. multiobjective evolutionary algorithm based on decomposition (MOEA/D) [28], multiobjective multiverse optimizer (MOMVO) [29], multiobjective salp swarm algorithm (MSSA) [30], multiobjective Pareto-based firefly algorithm (pb-MOFA) [31], multiobjective flower pollination algorithm (MOFPA) [32], nevMOGA algorithm [33], and Multi-objective particle swarm optimization (MOPSO) [34]. In Ref. [35], the optimal capacitor placement problem is solved by fuzzy logic decision and bacteria foraging algorithm (BFA) in 34-bus RDN. The objective is to reduce the cost of peak power and energy loss and enhance the voltage profile. Fuzzy logic is used to identify the installation node. The BFA is applied to determine the optimal locations and sizes of capacitors. Comparisons with other optimizer show that BFA achieves a more economical solution by minimizing the total injected VAr into the system, power losses, energy loss, and enhancing the voltage profile. In Ref. [36], the capacitor allocation problem is formulated as a multiobjective problem purposing to reduce real power loss, capacitor costs, and voltage deviation, and raise the capacity limit of the feeders and the transformer. A two-stage immune algorithm is proposed to solve the multi-objective optimal capacitor allocation problem using compromise programming. Fuzzy sets are used that reflect the imprecise nature of objectives. The Pareto optimal solutions are determined by this algorithm. The comparisons with other optimizers in the literature indicate that this method yields encouraging results that prove the effectiveness of this method. In Ref. [37], multi-objective optimal allocation of distributed generation and shunt capacitors in 33-bus and Indian 85-bus systems for reduction of real power loss and voltage deviation is proposed. The optimization problem is solved by the hybrid WIPSO–GSA algorithm which is weight improved particle swarm optimization (WIPSO) hybridized with gravitational search algorithm (GSA). First, the fixed-sized archive is used to save the Pareto front. Then, a leader selection strategy is applied to determine the best compromise among Pareto optimal solutions. The findings show the superiority of hybrid WIPSO–GSA when comparing the results with other optimizers. In Ref. [38], multi-objective optimization of optimal capacitor placement is determined along radial distribution networks; IEEE 34-bus and 118-bus systems. The target is to improve the total voltage stability index, reduce power loss, and boost annual net savings. Load sensitive factor is used to determine the most effective locations to place the capacitors. Then, multi-objective optimization using GA is applied to determine the optimal allocation of capacitors. The simulation results show that the proposed approach effectively enhances the total voltage stability index, reduces power loss, and maximizes annual net savings.

A Fast and elitist nondominated sorting genetic algorithm II (NSGA-II) is an advanced issuance of NSGA [39,40]. The NSGA-II has been tested for difficult problems but exhibits its ability to preserve better diversity among solutions and achieves good convergence close to the true Pareto-optimal solutions in comparison with two other elitist multiobjective evolutionary algorithms (MOEAs) i.e. Pareto-archived evolution strategy (PAES) and strength-Pareto EA (SPEA) [40]. In particular, a genetic algorithm (GA) can solve complex problems with characteristics such as discontinuous, nonconvex, and multimodal solutions spaces which motivate authors to propose it [41]. Multiobjective grey wolf optimizer (MOGWO) is an updated version of grey wolf optimizer (GWO) to tackle multi-objective problems. GWO mimics the hunting behavior of grey wolves according to the social hierarchy. Comparisons with prominent meta-heuristics, multiobjective evolutionary algorithm based on decomposition (MOEA/D), and multi-objective particle swarm optimization (MOPSO), have revealed that MOGWO has a good convergence behavior and significant superior results [42]. The multiobjective water cycle algorithm (MOWCA) simulates the water cycle mechanism in nature including evaporation, raindrops, and the rushing water from rivers and streams towards the sea. Compared to other optimizers, MOWCA has proven to be a promising tool in giving competitive results along with its robustness and steadily convergence to solve nonconvex problems with different levels of difficulty [26].

The major contributions of this manuscript are to tackle the multi-objective allocation problem of fixed and switched capacitors to enhance the overall voltage stability index and boost the annual net savings taking into account the operating system constraints. The fuzzy logic is utilized to specify the nominee nodes for capacitor allocation. The voltage and normalized loss sensitivity factor LSF_{norm} are utilized as inputs for fuzzy expert rules. NSGA-II based fuzzy decision maker is then used to calculate the best locations and sizes of capacitors. To test the effectiveness of the suggested method, it is applied to IEEE 33-bus and actual Portuguese 94-bus RDNs. To test the feasibility of the applied method, comparisons are made with other algorithms such as MOWCA and MOGWO with other challenging methods from published papers, namely, the interior point algorithm and the combination fuzzy-real coded GA algorithm for 33-bus system and artificial bee colony algorithm for 94-bus system.

The rest of this manuscript is arranged as follows, Section 2 formulates the problem. Section 3 explains the LSF. Section 4 displays the fuzzy expert rules. Section 5 presents with details the NSGA II and fuzzy decision maker. Section 6 shows the results and analysis. Section 7 concludes the manuscript. Section 8 presents the future work.

2. Problem formulation

In traditional optimization methods, the multiobjective optimization problem (MOP) is turned into one objective problem by the weighting factor to obtain the best solution based on the suggested value of the weighting factor.

Many problems include optimization of many conflicting targets concurrently. MOPs produce a set of nondominated solutions termed as the Pareto-optimal solutions. Among all Pareto-optimal solutions, no solution can be regarded as optimal without proper judgment [43].

A vector objectives optimization problem is composed of several conflicting objectives subject to certain constraints. Without loss of generality, the multivector objectives can be mathematically defined as follows [26]:

$$Minimize \left\{\overrightarrow{F_m(\vec{x})}\right\}, \forall m \in N_{obj} \ and \ \vec{x} \in set \ of \ constraints \tag{1}$$

where, N_{obj} is the number of objective functions; x is a decision vector representing a possible solution;

For MOP, suppose there are two solutions $\vec{x}$ and $\vec{y}$. Any of two prospects can happen to any solution, one solution dominates the other or does not dominate the other. In a minimization problem, $\vec{x}$ dominates $\vec{y}$ if:

$$F_i(\vec{x}) \leq F_i(\vec{y}), \forall i \in N_{obj} \tag{2}$$

and

$$F_j(\vec{x}) \leq F_j(\vec{y}), \forall j \in N_{obj} \tag{3}$$

If the above conditions are achieved, $\vec{x}$ is known as a nondominated solution. $\vec{x}$ represents a Pareto-optimal solution if no other solution is discovered to dominate $\vec{y}$. A set of Pareto-optimal solutions is called a Pareto-optimal front. In MOP, if there are two or more objectives that should be optimized simultaneously, then the greedy selection procedure is applied according to a dominance-based filter [43].

2.1. Annual net savings

The objective is to boost the net savings/year by minimizing the peak active power loss and the capacitor costs, and it is specified in (4) as,

$$F_1 = K_e \times (P_{La} - P_{Lb}) \times T + \alpha \times \left[C_i \times N_B + C_P \times \sum_{i=1}^{N_B} Q_c(i)\right] + C_O \times N_B \tag{4}$$

Where, K_e, C_i, C_P, and C_O represent energy cost, installation expenses, purchase expenses of the capacitor, and capacitor operating cost, respectively; P_{Lb} and P_{La} represent the overall active power losses at base case and after reactive compensation, respectively. α is a depreciation coefficient. T is the time interval. N_B is the total number of buses where the capacitors are installed; $Q_C(i)$ is reactive power injected at node i [44]. The annual net savings are defined as [45]:

$$S = minimization \ of \ energy \ cost - \alpha \times [installations \ cost + purchase \ cost] - operating \ cost/year \tag{5}$$

2.2. Voltage stability index (VSI)

VSI is employed to indicate the stability level in RDNs and thereby there will be an appropriate action if VSI shows a poor value. VSI ranges from zero at a point of voltage collapse to unity at no load. The node with a minimum value of VSI has the greatest chance of voltage collapse [46,47] and the voltage collapse condition will appear at that node. Thus, supplying the appropriate nodes with reactive power support can help improving voltage stability [46]. The total voltage stability index (TVSI) can be determined by (6) whereas VSI at bus j is expressed using (7) [43]. Fig. 1 depicts a simple distribution line $i-j$.

$$TVSI = \sum_{j=2}^{N} VSI[j] \tag{6}$$

$$VSI[j] = |V[i]|^4 - 4 \times \left(P_{eff}[j] \times R_{ij} + Q_{eff}[j] \times X_{ij}\right) \times |V[i]|^2 - 4 \times \left(P_{eff}[j] \times X_{ij} - Q_{eff}[j] \times R_{ij}\right)^2 \tag{7}$$

Where N is the total number of buses; $V[i]$ represents the voltage magnitude of sending end node i; $P_{eff}[j]$ and $Q_{eff}[j]$ are effective real and reactive powers at the receiving end bus j, respectively; R_{ij} and X_{ij} are resistance and reactance of branch $i-j$, respectively.

The objective function suggested to maximize the *TVSI* is written by:

$$F_2 = \frac{1}{TVSI} \tag{8}$$

2.3. Objective function

A multiobjective optimization procedure is applied for optimal capacitor allocation problem in RDNs. In this study, two objectives are planned for simultaneous optimization. They are (1) (S) maximization and (2) (TVSI) maximization whereas fulfilling all operating system constraints. The vector of objectives that have to be reduced concurrently can be defined in (9).

$$minimize : \{F_1; F_2\} \tag{9}$$

2.4. System constraints

1. Power balance constraints:

$$P_{Slack} = \sum_{i=1}^{n_l} P_D[i] + \sum_{j=1}^{n} P_L[j] \tag{10}$$

$$Q_{Slack} + \sum_{i=1}^{N_B} Q_C[i] = \sum_{i=1}^{n_l} Q_D[i] + \sum_{j=1}^{n} Q_L[j]$$

where, P_{Slack} and Q_{Slack} represent real and reactive powers provided by slack bus, respectively; $P_D[i]$ and $Q_D[i]$ represent active and reactive demands of bus i, respectively; $P_L[j]$ and $Q_L[j]$ represent active and reactive losses at section j, respectively; n_l and n are the numbers of PQ buses and

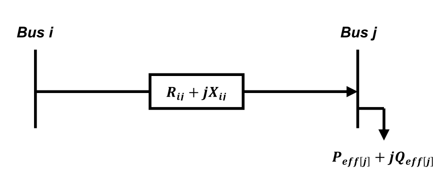

Fig. 1. A model of distribution line.

branches, respectively [45];

2. Voltage limits:

$$V_{min} \le |V[i]| \le V_{max} \tag{11}$$

where, V_{min} and V_{max} are the lower and upper bounds of voltage profile, respectively.

3. Distribution line capacity constraints:

$$S[i] < S[i]^{rated} \tag{12}$$

where, $S[i]^{rated}$ denotes the allowable maximum rating at line section i [16].

4. Capacitor size constraint:

$$Q_c^{min} \le |Q_c[i]| \le Q_c^{max} \tag{13}$$

where, Q_c^{min} and Q_c^{max} are the permissible lower and upper limits of the reactive power injection at any candidate bus.

5. Total injection constraints [45]:

$$\sum_{i=1}^{N_B} Q_C[i] \le \sum_{j=1}^{n_l} Q_D[j] \tag{14}$$

3. Loss sensitivity factor (LSF)

As depicted in Fig. 1, real power loss in section ij is formulated as:

$$P_{lineloss}[ij] = \frac{\left(P_{eff}^2[j] + Q_{eff}^2[j]\right) \times R_{ij}}{V^2[j]} \tag{15}$$

Where, $V[j]$ represents the voltage at location j.

LSF can be determined by Ref. [48]:

$$LSF[j] = \frac{\partial P_{lineloss}[ij]}{\partial Q_{eff}[j]} = \frac{2 \times Q_{eff}[j] \times R_{ij}}{V^2[j]} \tag{16}$$

LSF values are normalized to be modelled by fuzzy rules and LSF_{norm} can be obtained by:

$$LSF_{norm}[j] = \frac{LSF[j] - LSF_{min}}{LSF_{max} - LSF_{min}}, j\forall[2, N] \tag{17}$$

LSF_{norm} varies from 0 to 1 [43]. The buses with maximum LSF_{norm} values are more sensitive to place the capacitors [48].

4. Fuzzy expert system (FES)

Table 1 shows the fuzzy decision matrix summarizing the fuzzy rules [43]. The rows and columns of the fuzzy decision matrix represent two inputs, the voltage $|v_i|$ and LSF_{norm}, and they are coupled with IF parts in the IF-THEN rules. The suitability, a third-dimensional variable, is the conclusion that lies at the cross point of each row and each column, and that output is related to the THEN part in IF-THEN rules [43,49]. FES calculates the suitability of all nodes using a set of heuristic rules. Then, the highly nominated nodes for capacitor allocation are determined according to buses with the largest suitability values [43]. The fuzzy rule comprises twenty-five if-then rules to derive the conclusion or control output as listed in Table 1.

The fuzzy terms, Low, Low- Medium/Normal, Medium/Normal, High- Medium/Normal, and High, are used to describe the fuzzy variables, voltage, LSF_{norm}, and capacitor placement suitability. Triangular and trapezoidal membership functions (MFs) are suggested. The centroid method is utilized for defuzzification. Figs. 2–4 graphically depict the MFs. Fig. 5 displays the surface chart of these rules.

The initial selection of the most nominated nodes for capacitor allocation has helped in reducing the search space for NSGA-II and consequently decreasing CPU processing time [43].

Table 1
Fuzzy expert rules for determining high nominated nodes.

AND		$\lvert v_i \rvert$				
		L	LN	N	HN	H
LSF_{norm}	L	LM	LM	L	L	L
	LM	M	LM	LM	L	L
	M	HM	M	LM	L	L
	HM	HM	HM	M	LM	L
	H	H	HM	M	LM	LM

5. A nondominated sorting genetic algorithm (NSGA II) based approach

The nondominated sorting genetic algorithm (NSGA) is a powerful technique to handle MOPs. It was first developed by Srinivas and Deb. NSGA faces three challenges 1) high computational complexity, 2) nonelitism, and 3) the necessity for identification of a sharing parameter. To tackle these difficulties, Deb et al. developed NSGA II. NSGA-II generates a number of fronts that reduce multiple objectives to a single fitness arranged based on nondomination [41,50].

5.1. Fast nondominated sorting approach

After initializing the population P_t of size N and determining the objective functions, two important entities for every solution p in population P_t have to be estimated: 1) domination count n_p, the number of individuals or solutions that dominate the individual p, and 2) the set of individuals S_p that is dominated by individual p.

If solution p dominates solution q in the population P_t, then add solution q to a set of individuals S_p. If solution q dominates solution p, then increase n_p by one. If no solution dominates solution p ($n_p = 0$), then p belongs to the first front F_1 with rank = 1.

After identifying the first front F_1, the front counter is initialized (i = 1) to determine the nonempty front F_i. A discrete list Q is initialized to arrange the solutions of the next fronts. For every individual p in F_i, every member q in its set S_p will be visited thereby decreasing domination count n_q for member q by one. When domination count n_q for any member q is zero, this member is directly carried over to a discrete list Q belonging to the second nondominated front F_2 with rank = 2. This procedure continues to find all fronts [40,41].

In second or higher nondominated levels, the domination count for each solution p is at most $N-1$. Therefore, every solution p is visited mostly $N-1$ until n_p reaches zero. As soon as the domination count n_p for any solution becomes zero, this individual is assigned a nondomination level, and it is not permissible to visit this solution again. The total complexity for the procedure is $O(MN^2)$, where M is a number

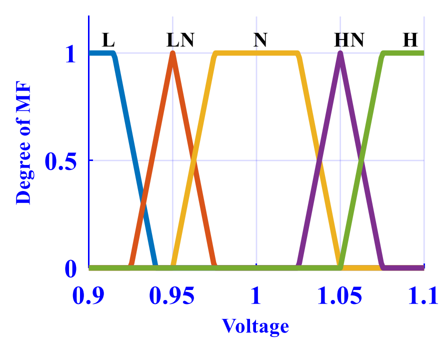

Fig. 2. MFs for voltage.

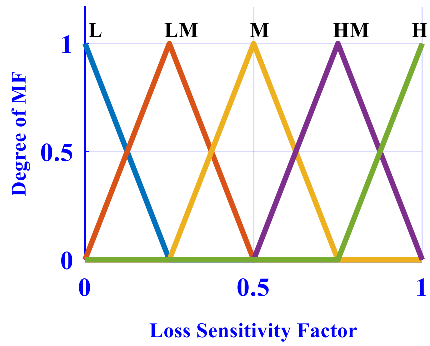

Fig. 3. MFs for LSF_{norm}

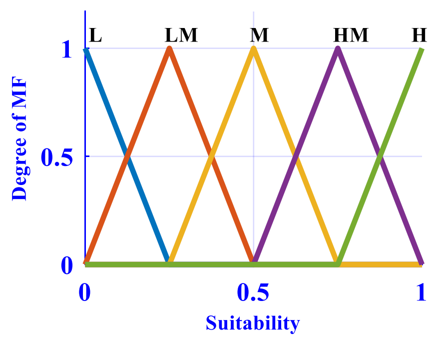

Fig. 4. MFs for suitability.

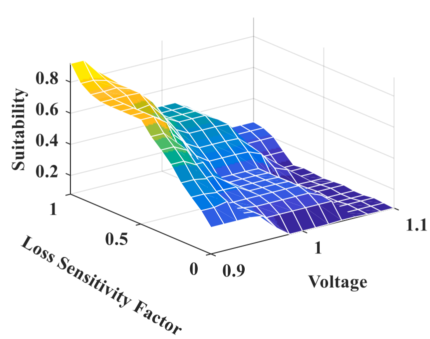

Fig. 5. The surface chart of fuzzy expert rules.

of objective functions and N is a population size.

5.2. Density estimation

In order to determine the spread of individuals around a particular individual in the population, the mean separation of two points on each side of this point along every objective is determined. The crowding distance C_rD is estimated to be the perimeter of the cuboid shaped by the closest neighbours as the vertices.

To calculate C_rD, this needs arranging the population P_t into each front based on each function value in ascending sort. For every function, an infinite distance value is specified for boundary solutions. The C_rD of all other intermediate solutions is set as the absolute normalized difference in the objective function values of two adjoining individuals. The total C_rD is computed as the sum of all distance values for every function. Every objective function is normalized before determining the C_rD.

5.3. Crowded-comparison operator

The crowded-comparison operator directs the choice process towards uniformly spread-out Pareto-optimal solutions. To choose between two solutions belonging to different fronts ($p_{rank} \neq q_{rank}$), the preference is for a lower-ranked solution. On the other hand, if both solutions have the same nondomination rank ($p_{rank} = q_{rank}$), the preference is for the solution with a less crowded area.

5.4. Main loop

A random parent population is initially generated, and then it is arranged according to nondomination into each front. Every individual has a fitness (or rank) equal to its nondomination level [40]. Besides the rank, the crowding distance C_rD is determined for every solution to estimate how close each solution is to its adjoining. The crowded-comparison operator is introduced to select the parents according to rank and crowding distance [41]. The selection, crossover, and mutation operators [41] are implemented to generate an offspring population Q_t of size N. An elite-conserving operator is introduced making the best solutions in the population move directly to the next generation. Therefore, the good solutions discovered early are maintained as long as a better solution is not yet found.

First, a combined population R_t of size $2N$ is obtained as $R_t = P_t \cup Q_t$. Population R_t is then organized according to nondomination. Since population R_t comprises all former and present members of the population, elitism is achieved. Now, the best individuals in R_t are the individuals of the best nondominated set F_1. If the size of F_1 is less than N, its members are selected for the new population P_{t+1}. All other individuals of the population P_{t+1} are picked from suffix nondominated fronts according to their ranking. Therefore, individuals from set F_2 are selected next, then from set F_3, and so on. This procedure ends as soon as no other set can be accommodated. To select exactly all members in the population N, the individuals in the last nondominated front F_l are arranged by the crowded-comparison operator in descending sort [40]. The best-required individuals are picked to fill all slots in the population. The selection, crossover, and mutation operators [41] are employed to create a new population Q_{t+1} of size N [40].

5.5. Fuzzy decision maker (FDM)

After a Pareto front is produced, the optimal solution is picked by the decision maker (DM) according to worth decisions and good judgments among Pareto-optimal solutions. The fuzzy satisfactory technique may be helpful in that problem. A linear waveform is elicited for fuzzy membership functions as depicted in Fig. 6. Linear membership function μ_i can be mathematically formulated by:

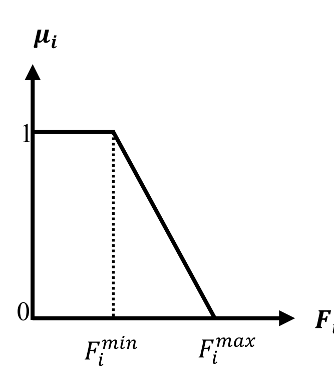

Fig. 6. Linear membership function.

$$\mu_i = \begin{cases} 1, if F_i \le F_i^{min} \\ \dfrac{F_i^{max} - F_i}{F_i^{max} - F_i^{min}}, if F_i^{min} < F_i < F_i^{max} \\ 0, if F_i \ge F_i^{max} \end{cases} \tag{18}$$

Where, F_i is the value of objective function i; Here $\mu_i = 0$, FDM is fully unsatisfied; whereas $\mu_i = 1$, FDM is fully satisfied.

The normalized membership function μ^k can be defined for any optimal Pareto solution k using (19):

$$\mu^k = \frac{\sum_{i=1}^{N_{obj}} \mu_i^k}{\sum_{k=1}^{M} \sum_{i=1}^{N_{obj}} \mu_i^k} \tag{19}$$

where, N_{obj} is the objective function number; M is the number of Pareto front's members.

The solution with the highest value of μ^k is picked as the best compromise solution [51]. Fig. 7 shows the flowchart of the NSGA-II

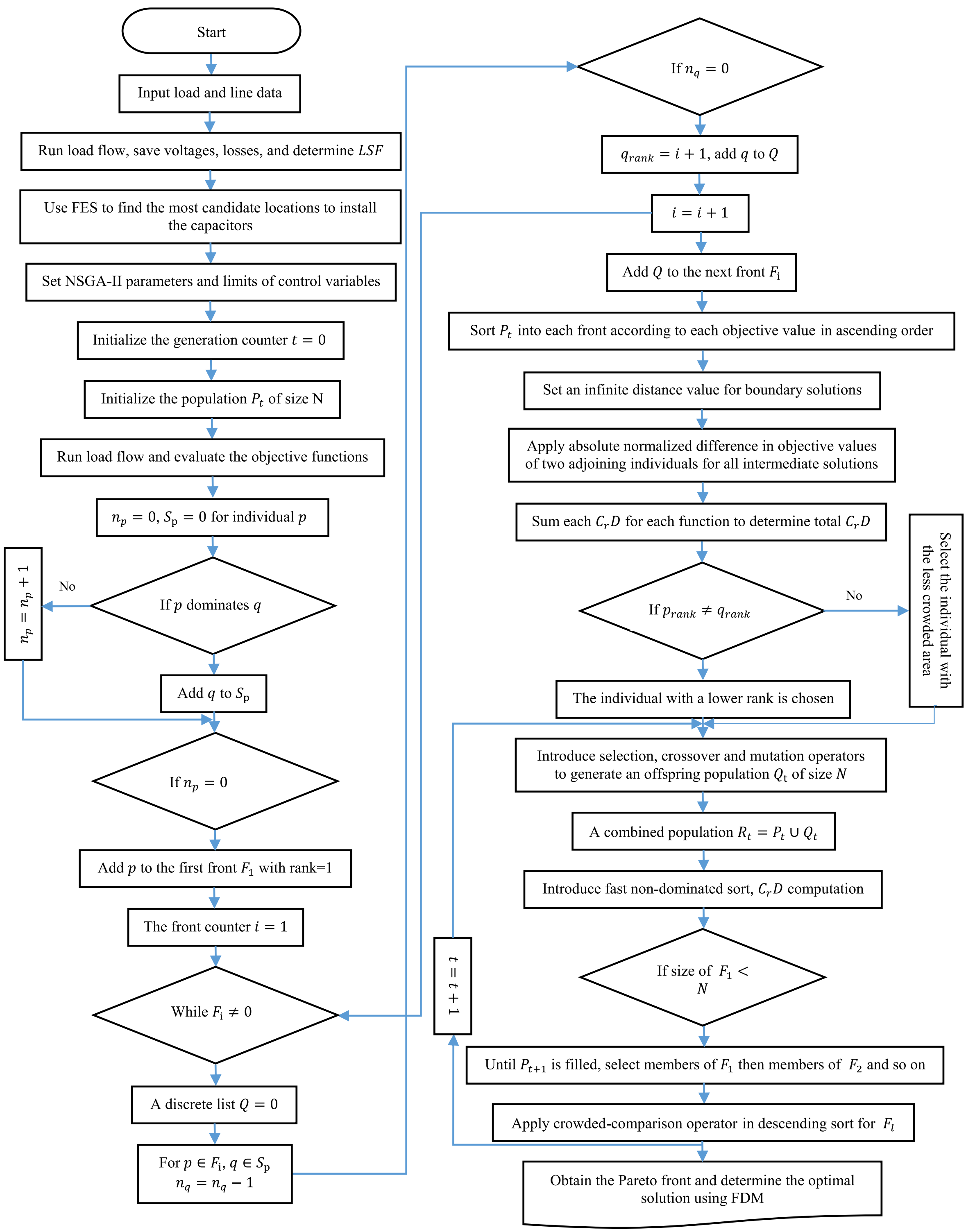

Fig. 7. Flowchart of NSGA-II based approach.

based approach.

6. Numerical results and discussions

To emphasize the validity and capability of the proposed methodology to solve the optimal capacitor allocation problem, numerical simulations are applied to IEEE 33- bus and an actual Portuguese IEEE 94-bus RDNs. The bus-injection to branch-current (BIBC) and branch-current to bus-voltage (BCBV) matrices [52] are implemented to solve the load flow (LF) for the proposed RDNs.

The proposed algorithm and the LF solution are programmed in the MATLAB environment with Intel(R) Core (TM) i3-3217U CPU, 1.80 GHz, a 4.0 GB RAM Dell laptop, and a 64- bit operating system. For all test cases, the constant values used to determine net savings per year are set as: $K_e = \$0.06/\text{kWh}, C_i = \$1600/\text{location}, \ C_p = \$25/\text{kVAr}, C_o = \$300/\text{year}/\text{location}, \ \alpha = 20\%, T = \text{Hours } 8760 \ /\text{year}$ [44]. The voltage constraint is assumed from 0.91 to 1.1 p.u. for 33- node system, while the voltage constraint is from 0.9 to 1.1 p.u. for 94- node system. The control variables representing the ratings of fixed and switched capacitors are between the lower limit (50 kVAr) and the upper limit (1500 kVAr). The control variables of fixed capacitors are randomly distributed throughout the search space [4], while in switched capacitors, these values are distributed from the lower limit to the upper limit by a fixed step of 50 kVAr [45].

The calculation of most candidate buses for capacitor placement can help in minimization of the search space for the proposed NSGA-II. By conducting many trials, it was concluded that 10–25% of the total number of system buses after being arranged are the optimal solutions or close to optimal solutions. For systems with small sizes like 33-node RDN, the user may pick 20–25% of system buses with the largest suitability values calculated by fuzzy expert rules as the initial possible locations for capacitor placement. While the user may select for large-scale systems (i.e 94-node RDN) 10–15% of system buses with the largest suitability values as the initial candidate locations for capacitor placement [45]. Certainly, fuzzy expert rules may not determine the optimal buses for capacitor allocation. This is due to the inputs to fuzzy rules are the voltage and loss sensitivity factor which depend on the system topology, configuration, and loading [45]. Thus, the proposed NSGA-II is applied to find the optimal sizes and locations for capacitor placement.

The comparisons are made with MOWCA, MOGWO, and other reported optimizers concerning voltage profile, active and reactive power losses, total voltage stability index, and net savings/year.

The control parameters of NSGA-II are set as: the distribution index for crossover operator $\eta_e = 20$, the distribution index for mutation operator $\eta_m = 20$, and the number of generations = 200.

The control parameters of MOWCA are adjusted as: population size $N_{pop} = 150$, number of rivers and sea $N_{sr} = 25$, evaporation condition constant $d_{max} = 10^{-16}$, and number of iterations is 150 for 33-bus RDN and 300 for 94-bus RDN.

The MOGWO parameters are set as: grid inflation parameter $\alpha = 0.1$, leader selection pressure parameter $\beta = 4$, number of grids per each dimension nGrid = 10, and number of iterations is 100 for 33-bus RDN and 200 for 94-bus RDN.

Two case studies are used to verify the efficacious of a two-stage methodology.

1. Optimal placement of fixed capacitors.
2. Optimal placement of switched capacitors

6.1. 33-bus RDN

This system contains 33 buses and 32 lines. The line and bus data can be obtained from Ref. [53]. Fig. 8 shows the network layout of 33-bus RDN. The total real and reactive power demands are 3715 kW and 2300 kVAr, respectively. The per-unit system is used in simulation with base values $V_{Base} = 12.66$ kV and $S_{Base} = 10$ MVA. The nine top-ranking buses (i.e 20–25% of system buses) are picked as the initial potential locations for capacitor placement according to fuzzy expert rules; $\{28, 6, 29, 8, 30, 9, 13, 10, 3\}$.

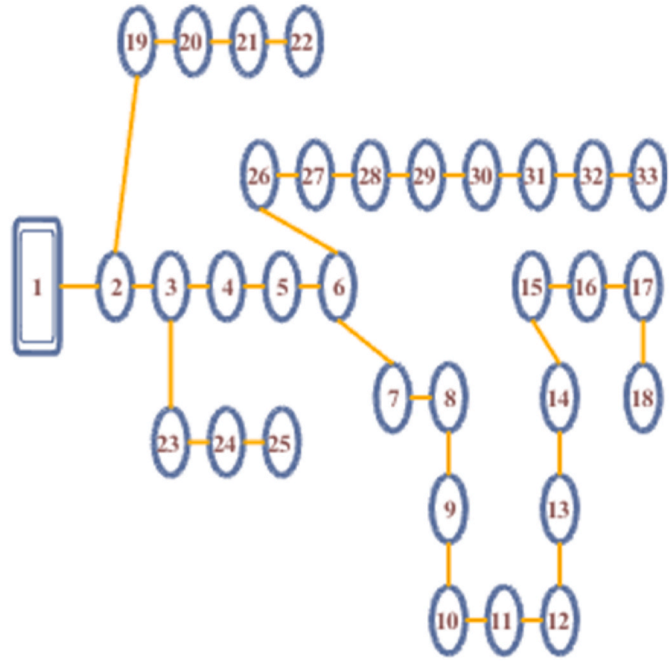

Fig. 8. Network layout of 33-bus RDN.

Table 2 displays the optimum buses and capacities for fixed and switched capacitors using NSGA-II against two optimizers; MOWCA and MOGWO and other optimizers obtained from literature, FRCGA [46] and IP algorithm [54]. NSGA–II– fixed selects four capacitors at bus numbers $\{6, 8, 30, 13\}$ with ratings of $\{137, 359, 1035, 430\}$ kVAr while NSGA–II– switched picks three capacitors at bus numbers $\{30, 13, 10\}$ with ratings of $\{1150, 350, 400\}$ kVAr, respectively.

Table 3 gives the results before compensation and after using NSGA-II against MOWCA, MOGWO, and other techniques found in the literature. This Table lists V_{min} (p.u), V_{max} (p.u), $\sum P_{Loss}$ (kW), Reductions in P_{Loss} (%), $\sum Q_{Loss}$ (kVAr), Reductions in Q_{Loss} (%), VSI_{min}, VSI_{max}, TVSI, and Net Savings/year.

From Tables 2 and 3, NSGA-II reduces power losses from 210.998 kW + j143.033 kVAr to 142.7004 kW + j 97.5605 kVAr using fixed capacitors and 145.3756 kW + j99.4153 kVAr using switched capacitors with lower injected kVArs of 1961 kVAr and 1900 kVAr which are better than 150.6170 kW + j103.4236 kVAr and 149.9388 kW + j103.7441 kVAr of MOWCA, 148.7872 kW + j102.0343 kVAr and 146.2804 kW + j 100.3518 kVAr of MOGWO, 148.6951 kW of FRCGA, and 171.78 kW of IP algorithm with injected kVArs of 2087 kVAr, 2150 kVAr, 2035 kVAr, 2050 kVAr, 2250 kVAr, and 2150 kVAr for MOWCA-fixed, MOWCA-switched, MOGWO-fixed, MOGWO switched, FRCGA, and IP algorithm, respectively. It is observed from load flow results that the end buses have lower voltages owing to the presence of heavy inductive loads. The lowest voltage without capacitor placement is 0.9039 p.u at bus number 18. After installing capacitors, the voltages are substantially improved due to the compensation of a portion of reactive power absorbed by loads. The minimum voltages using NSGA-II are 0.9412 p.u and 0.9425 p.u which are less than 0.9472 p.u and 0.9484 p.u using MOWCA, 0.9456 p.u and 0.9446 p.u using MOGWO, 0.9665 p.u using FRCGA, and 0.9501 p.u using IP algorithm. TVSI is enhanced from 25.5401 to 27.8320 and 27.8800 using NSGA-II which are lower than 28.1298 and 28.1519 using MOWCA and 28.0545 and 28.0080 using MOGWO. NSGA-II results in annual net savings of 23,612$ and 23,131$ for fixed

Table 2
Optimum buses and capacities for 33-bus RDN for the two cases.

Item	NSGA-II		MOWCA		MOGWO		Fuzzy-real coded GA algorithm (FRCGA) [46]	Interior point algorithm (IP) [54]
	Fixed	Switched	Fixed	Switched	Fixed	Switched		
Capacitor locations	6, 8, 30, 13	30, 13, 10	30, 13, 10	8, 30, 13	30, 13, 10	8, 30, 13	28, 6, 29, 8, 30, 9	9, 29, 30
Capacitor Sizes (kVAr)	137, 359, 1035, 430	1150, 350, 400	1211, 396, 480	650, 1000, 500	1199, 362, 474	400, 1150, 500	100, 325, 425, 350, 675, 375	450, 800, 900
Total kVAr	1961	1900	2087	2150	2035	2050	2250	2150

Table 3
The results before and after proposing capacitors for 33-bus RDN.

Item	Base case	NSGA-II		MOWCA		MOGWO		FRCGA [46]	Interior point algorithm (IP) [54]
		Fixed	Switched	Fixed	Switched	Fixed	Switched		
V_{min} (p.u)	0.9039 @bus 18	0.9412	0.9425	0.9472	0.9484	0.9456	0.9446	0.9665	0.9501
V_{max} (p.u)	0.9970 @bus 2	0.9977	0.9976	0.9977	0.9977	0.9977	0.9977	–	–
$\sum P_{Loss}$ (kW)	210.998	142.7004	145.3756	150.6170	149.9388	148.7872	146.2804	148.6951	171.78
Reductions in P_{Loss} (%)	–	32.3690	31.1011	28.6170	28.9384	29.4842	30.6722	29.5278	18.5870
$\sum Q_{Loss}$ (kVAr)	143.033	97.5605	99.4153	103.4236	103.7441	102.0343	100.3518	–	–
Reductions in Q_{Loss} (%)	–	31.7916	30.4948	27.6924	27.4684	28.6638	29.8401	–	–
VSI_{min}	0.6672 @bus 18	0.7848	0.7890	0.8050	0.8091	0.7996	0.7961	0.8652	–
VSI_{max}	0.9881 @bus 2	0.9906	0.9906	0.9908	0.9908	0.9907	0.9907	–	–
TVSI	25.5401	27.8320	27.8800	28.1298	28.1519	28.0545	28.0080	–	–
Net Savings/year	–	23,612	23,131	19,441	19,483	20,663	21,906	17,777	8003.2

and switched capacitors, respectively, which are higher than 19,441$ and 19,483$ of MOWCA, 20,663$ and 21,906$ of MOGWO, 17,777$ of FRCGA, and 8003.2$ of IP algorithm. The operating system constraints have been confirmed and have not exceeded the permissible limits. It's estimated that the CPU time needed to finish one optimization run is 122 s for the NSGA-II, 428 s for MOWCA, and 212 s for MOGWO. It is well-known that the optimization time includes the time spent in the load flow and may reach 70–75% of the optimization time.

Figs. 9–11 depict the best compromise among Pareto optimal solutions by NSGA-II, MOWCA, and MOGWO, respectively. Fig. 12 shows the voltages comparison without and with fixed and switched capacitors using the NSGA-II, MOWCA, and MOGWO. The voltage profile is also depicted by the increased TVSI. Although the total power losses, annual net savings, and total compensated power using NSGA-II are better than those found in other techniques, yet the minimum voltage and TVSI using NSGA-II are less than those obtained by other methods. The better performance of NSGA-II than its counterparts is reflected in its superiority in achieving the highest annual net savings, which adds greater value to this method.

6.2. An actual Portuguese 94-bus RDN

To test the strength of NSGA-II when applied to large radial distribution networks, 94 buses are selected. Fig. 13 shows the network layout of 94-bus RDN. The whole description of this system, including load and line data, can be found in Ref. [55]. It comprises 94 buses and 93 lines, where the rated voltage is 15 kV and total demands are 4797 kW and 2323.9 kVAr. It should be noted that minimum voltages at the base case do not respect the permissible upper and lower limits. This is due to its presence in a rural region and the demanding attributes of the network that enforce difficult operating conditions. The fifteen top-ranking nodes (i.e 10–15% of system buses) are selected as initial candidate buses for capacitor allocation according to fuzzy expert rules; 11, 90, 10, 18, 21, 54, 52, 15, 83, …,.

Table 4 lists the optimal buses and ratings of capacitors determined by NSGA-II against two optimizers; MOWCA and MOGWO and another optimizer obtained from the literature; ABC algorithm [45]. NSGA–II–fixed yields five locations for capacitor placement at bus numbers $\{11, 54, 83, 20, 23\}$ with sizes of $\{421, 893, 61, 621, 324\}$kVAr, while NSGA–II– switched selects five locations for capacitor placement at bus numbers $\{11, 90, 18, 54, 83\}$ with sizes of $\{300, 100, 500, 850, 550\}$ kVAr.

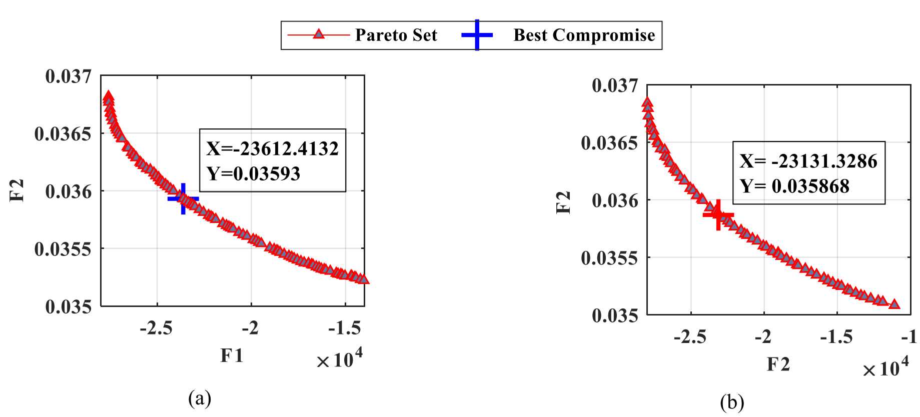

Fig. 9. Optimal solution among Pareto set for IEEE 33-node by NSGA-II for (a) fixed capacitors and (b) switched capacitors.

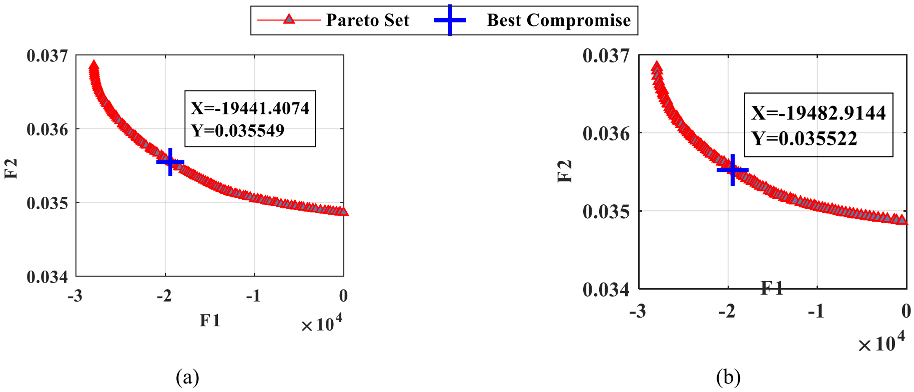

Fig. 10. Optimal solution among Pareto set for IEEE 33-node by MOWCA for (a) fixed capacitors and (b) switched capacitors.

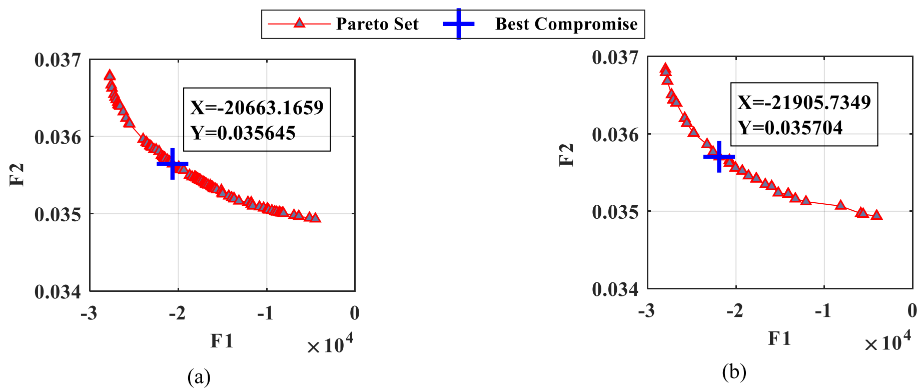

Fig. 11. Optimal solution among Pareto set for IEEE 33-node by MOGWO for (a) fixed capacitors and (b) switched capacitors.

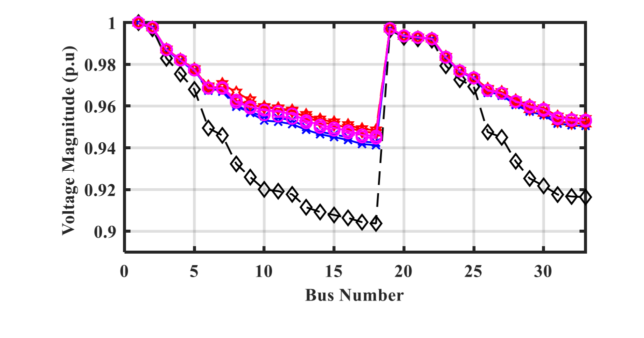

Fig. 12. Voltage profile comparison for 33- bus RDN at the base case and after capacitor installation.

Table 5 arranges the cropped results from the base case and with NSGA-II against MOWCA, MOGWO, and ABC algorithm [45]. In this table, V_{min} (p.u), V_{max} (p.u), $\sum P_{Loss}$ (kW), Reductions in P_{Loss} (%), $\sum Q_{Loss}$ (kVAr), Reductions in Q_{Loss} (%), VSI_{min}, VSI_{max}, TVSI, and Net Savings/year are summarized. NSGA-II can minimize total active power loss from 362.86 kW to 269.8589 kW and 271.0450 kW with Reductions in P_{Loss} (%) of 25.6296% and 25.3027% for fixed and switched capacitors, respectively, which are better than 274.8324 kW, 276.4410 kW, 272.4593 kW, 273.8650 kW, and 271.3590 kW with Reductions in P_{Loss} (%) of 24.2589%, 23.8156%, 24.9129%, 24.5255%, and 25.23% using MOWCA-fixed, MOWCA-switched, MOGWO-fixed, MOGWO switched, and ABC algorithm, respectively. NSGA-II reduces total reactive power loss from 504.04 kVAr to 373.2646 kVAr and 373.9985 kVAr with Reductions in Q_{Loss} (%) of 25.9457% and 25.8001% for fixed and switched

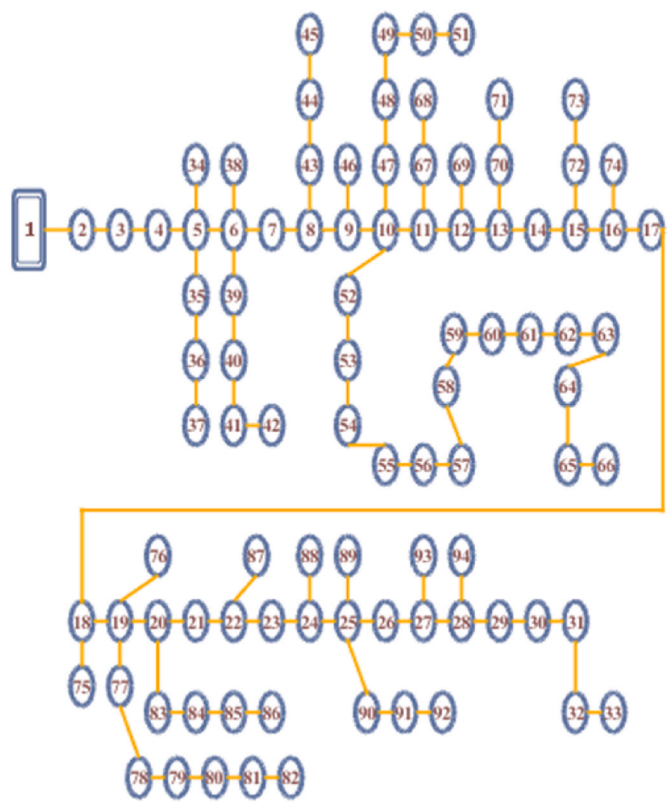

Fig. 13. Network layout of 94-bus RDN.

Table 4
Optimum buses and capacities for 94-bus RDN for the two cases.

Item	NSGA-II		MOWCA		MOGWO		ABC algorithm [45]
	Fixed	Switched	Fixed	Switched	Fixed	Switched	
Capacitor locations	11, 54, 83, 20, 23	11, 90, 18, 54, 83	54, 83, 16, 23	54, 20, 25	18, 54, 24	54, 15, 20	18, 21, 54
Capacitor Sizes (kVAr)	421, 893, 61, 621, 324	300, 100, 500, 850, 550	701, 584, 600, 437	800, 1200, 300	1000, 949, 369	750, 500, 1050	600, 450, 1050
Total kVAr	2320	2300	2322	2300	2318	2300	2100

Table 5
The results before and after proposing capacitors for 94-bus RDN.

Item	Base case	NSGA-II		MOWCA		MOGWO		ABC algorithm [45]
		Fixed	Switched	Fixed	Switched	Fixed	Switched	
V_{min} (p.u)	0.8485 @ bus 92	0.9150	0.9150	0.9200	0.9216	0.9168	0.9168	0.90721
V_{max} (p.u)	0.9951 @ bus 2	0.9972	0.9972	0.9972	0.9971	0.9972	0.9972	0.99699
$\sum P_{Loss}$ (kW)	362.86	269.8589	271.0450	274.8324	276.4410	272.4593	273.8650	271.3590
Reductions in P_{Loss} (%)	–	25.6296%	25.3027%	24.2589%	23.8156%	24.9129%	24.5255%	25.23%
$\sum Q_{Loss}$ (kVAr)	504.04	373.2646	373.9985	378.0763	380.3276	375.9245	376.6280	374.5060
Reductions in Q_{Loss} (%)	–	25.9457%	25.8001%	24.9911%	24.5445%	25.4180%	25.2785%	25.70%
VSI_{min}	0.5183 @ bus 92	0.7008	0.7010	0.7163	0.7215	0.7064	0.7066	0.6774
VSI_{max}	0.9804 @ bus 2	0.9887	0.9886	0.9887	0.9886	0.9887	0.9886	0.9879
TVSI	62.2650	75.5046	75.4905	76.1385	76.1747	75.7373	75.7710	75.0565
Savings/year	–	$34180	$33657	$32176.16	$32060.68	$34063	$33415	$35732

capacitors, respectively, which are better than 378.0763 kVAr, 380.3276 kVAr, 375.9245 kVAr, 376.6280 kVAr, 374.5060 kVAr with Reductions in Q_{Loss} (%) of 24.9911%, 24.5445%, 25.4180%, 25.2785%, and 25.70% using MOWCA-fixed, MOWCA-switched, MOGWO-fixed, MOGWO switched, and ABC algorithm, respectively. The lowest voltage at base case is 0.8485 p.u at bus number 92. The voltage profile is markedly improved after installing capacitors that inject reactive power into the system nodes. Therefore, the current flow and power losses are minimized. The lowest voltage after installing capacitors using NSGA-II is 0.915 p.u which is less than 0.92 p.u and 0.9216 p.u using MOWCA, and 0.9168 p.u using MOGWO. NSGA-II improves TVSI from 62.2650 to 75.5046 and 75.4905 which are lower than 76.1385 and 76.1747 using MOWCA and 75.7373 and 75.771 using MOWGO. NSGA–II–fixed yields annual net savings of 34,180 $ which are better than 33,657 $ using NSGA–II–switched, 32176.16 $ and 32060.68 $ using MOWCA, and 34,063 $ and 33,415 $ using MOGWO and are lower than 35,732 $ using ABC algorithm. The injected kVArs using NSGA-II are 2320 kVAr and 2300 kVAr, which are almost the same values for MOWCA of 2322 kVAr and 2300 kVAr and MOGWO of 2318 kVAr and 2300 kVAr and are slightly higher than 2100 kVAr using ABC algorithm. The higher injected kVArs add up to lower power losses and higher annual net savings. The improved performance of NSGA-II is shown by increased annual net savings. For all case studies, the operating system constraints have not exceeded the allowed boundaries. The time elapsed is 1024 s for NSGA-II, which is lower than 2849 s for MOWCA and 1204 s for MOGWO. Figs. 14–16 depict the best solution among Pareto optimal solutions using NSGA-II, MOWCA, and MOGWO, respectively. Fig. 17 indicates the network voltage profiles prior to and after capacitor installations using NSGA-II, MOWCA, and MOGWO. The voltage profile is greatly enhanced, which is demonstrated by high TVSI.

From these tables, for 33 bus system, fixed capacitors yield lower real power loss and higher annual net savings than those obtained from switched capacitors using NSGA-II, while switched capacitors achieve lower real power loss and higher annual net savings than those obtained from fixed capacitors using MOWCA and MOGWO. Fixed capacitors give lower reactive power loss than those obtained from switched capacitors using NSGA-II and MOWCA. Switched capacitors yield better TVSI than those obtained from fixed capacitors using the NSGA-II and MOWCA, while the fixed capacitors result in higher TVSI than those obtained from switched capacitors using MOGWO. For 94 bus system, fixed capacitors achieve lower active and reactive power losses and higher annual net savings than those obtained from switched capacitors using NSGA-II, MOWCA, and MOGWO. For TVSI, fixed capacitors give better results than those obtained from switched capacitors using NSGA-II, while switched capacitors yield better results than those obtained from fixed capacitors using MOWCA and MOGWO. Therefore, it can be concluded that fixed capacitors outperform switched capacitors in more results. This is due to the resilience of fixed capacitors to specify the values of

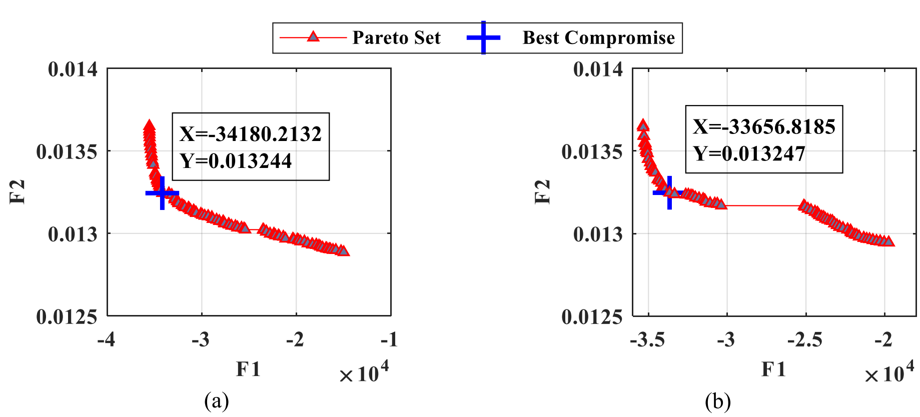

Fig. 14. Optimal solution among Pareto set for IEEE 94-node by NSGA-II for (a) fixed capacitors and (b) switched capacitors.

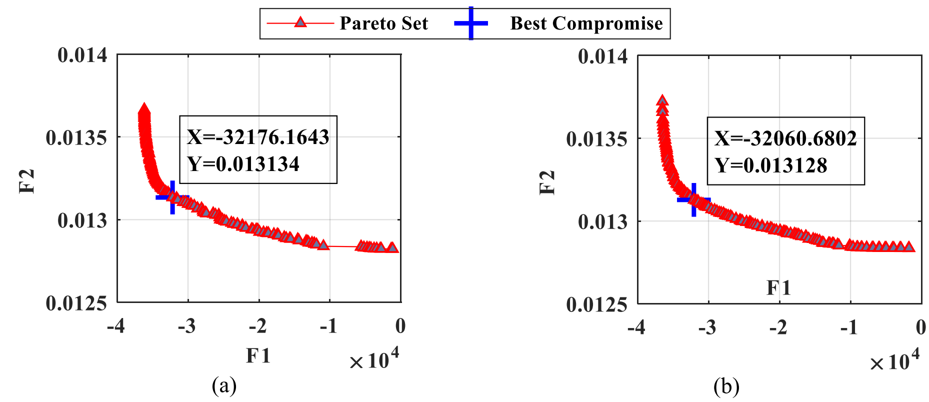

Fig. 15. Optimal solution among Pareto set for IEEE 94-node by MOWCA for (a) fixed capacitors and (b) switched capacitors.

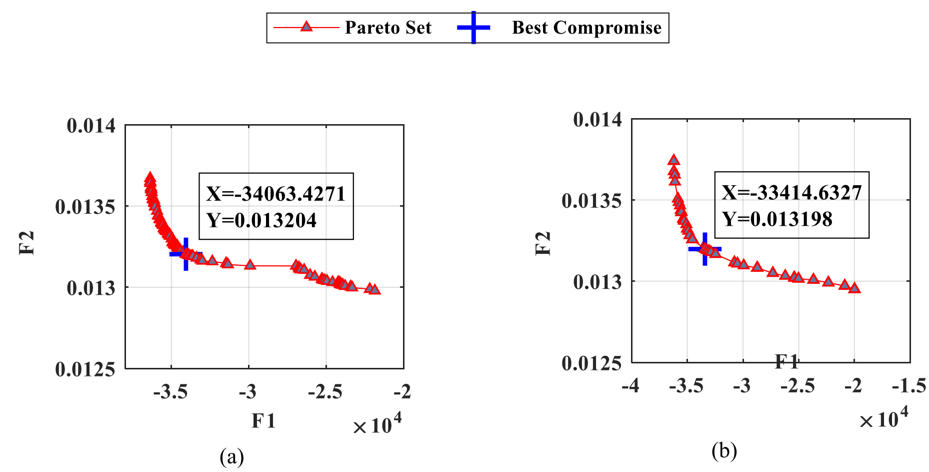

Fig. 16. Optimal solution among Pareto set for IEEE 94-node by MOGWO for (a) fixed capacitors and (b) switched capacitors.

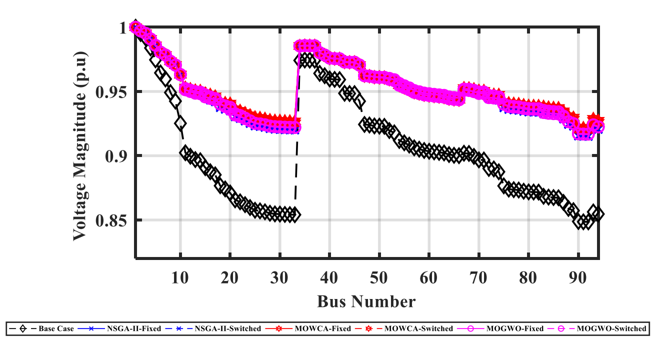

Fig. 17. Voltage profile comparison for 94- bus RDN at the base case and after capacitor installation.

control variables between lower and upper boundaries. While the control variables of switched capacitors are restricted to certain values between lower and upper boundaries.

7. Conclusions

This article discusses the optimal allocation of fixed and switched capacitors in radial distribution networks using NSGA-II. This problem is formulated considering multiple objectives to enhance voltage stability, reduce overall losses, and maximize total savings while satisfying all operating system constraints. Fuzzy logic is used to calculate the most candidate buses to be the optimal places for the capacitors. The NSGA-II based approach is then applied to calculate the optimal locations and sizes of the capacitors. IEEE 33-bus and actual Portuguese IEEE 94-bus RDNs are chosen to test the characteristics of this approach. The results from this method have been compared with the results found in MOWCA, MOGWO, and other algorithms found in published papers.

The results show that optimal capacitor allocation has improved system stability, reduced overall power losses, and maximized annual total savings, leading to enhanced network performance and reinforced system security. The proposed method has also proven its efficiency in giving high-grade solutions as well as its good convergence characteristics.

For the 33-node system, the percentages of minimization in real and reactive power losses using NSGA-II based approach are 32.369% and 31.7916% using fixed capacitors and 31.1011% and 30.4948% using switched capacitors. The annual total savings reach 23,612 $ and 23,131 $. The total voltage stability index is 27.832 using fixed capacitors and 27.88 using switched capacitors. For the 94-node system, the percentages of minimization in real and reactive power losses using NSGA-II based approach are 25.6296% and 25.9457% using fixed capacitors and 25.3027% and 25.8001% using switched capacitors. The annual total savings reach 34,180 $ and 33,657 $. The total voltage stability index is 75.5046 using fixed capacitors and 75.4905 using switched capacitors.

8. Future work

The future work is to add another parallel element to the capacitor for maximizing the results in terms of total voltage stability and net savings, which is a distributed generation. Hybridizing other optimizers with NSGA-II will be proposed to simultaneously determine optimal locations and sizes of multi-type distributed generations and capacitor banks in an unbalanced distribution system.

Credit author statement

Menna Allah El-sayed Mohamed El-Saeed: Conceptualization, Methodology, Software, Validation, Formal analysis, Investigation, Resources, Data curation, Writing- Original draft, Writing- Review and Editing, Visualization, Supervision, Project administration. **Amal Farouk Abdel-Gwaad.**: Conceptualization, Validation, Supervision, Resources, Data curation, and Project administration. **Mohamed AbdElfattah Farahat**: Conceptualization, Data curation, Validation, Supervision, Resources, Project administration.

Declaration of competing interest

The authors declare that they have no known competing financial interests or personal relationships that could have appeared to influence the work reported in this paper.

Data availability

The data that has been used is confidential.

References

[1] J.B. Bunch, R.D. Miller, J.E. Wheeler, Distribution system integrated voltage and reactive power control, IEEE Trans. Power Apparatus Syst. (2) (1982) 284–289, https://doi.org/10.1109/TPAS.1982.317104.

[2] M. Shahzad, Q. Shafiullah, W. Akram, M. Arif, B. Ullah, Reactive power support in radial distribution network using mine blast algorithm, Elektronika ir Elektrotechnika 27 (4) (2021) 33–40, https://doi.org/10.5755/j02.eie.28917.

[3] R.C. Dugan, M.F. McGranaghan, S. Santoso, H.W. Beaty, Electrical Power Systems Quality, McGraw-Hill Education, 2012.

[4] A.A. Abou El-Ela, R.A. El-Sehiemy, A. Kinawy, M.T. Mouwafi, Optimal capacitor placement in distribution systems for power loss reduction and voltage profile improvement, IET Gener., Transm. Distrib. 10 (5) (2016) 1209–1221, https://doi.org/10.1049/iet-gtd.2015.0799.

[5] H. Kaur, P. Kumar, A. Sharma, N. Kamaiya, A study on optimal capacitor placement in distribution system: conventional and Artificial Intelligence techniques, in: International Conference on Computation of Power, Energy, Information and Communication (ICCPEIC), IEEE, 2015, pp. 159–165, https://doi.org/10.1109/ICCPEIC.2015.7259457, 2015 .

[6] S.M. Parashar, G. Leena, M. Pande, J. Singh, Dynamic capacitor placement to mitigate disaster in distribution system: a fuzzy approach, in: International Conference on Power Electronics, Control and Automation (ICPECA), IEEE, 2019, pp. 1–5, https://doi.org/10.1109/ICPECA47973.2019.8975493, 2019 .

[7] J. Schmill, Optimum size and location of shunt capacitors on distribution feeders, IEEE Trans. Power Apparatus Syst. 84 (9) (1965) 825–832, https://doi.org/10.1109/TPAS.1965.4766262. .

[8] C.-S. Lee, H.V.H. Ayala, L. dos Santos Coelho, Capacitor placement of distribution systems using particle swarm optimization approaches, Int. J. Electr. Power Energy Syst. 64 (2015) 839–851, https://doi.org/10.1016/j.ijepes.2014.07.069. .

[9] B. Cao, et al., Spark-based parallel cooperative co-evolution particle swarm optimization algorithm, in: IEEE International Conference on Web Services (ICWS), IEEE, 2016, pp. 570–577, https://doi.org/10.1109/ICWS.2016.79, 2016.

[10] S. Kamel, M. Mohamed, A. Selim, L.S. Nasrat, F. Jurado, Power system voltage stability based on optimal size and location of shunt capacitor using analytical technique, in: 2019 10th International Renewable Energy Congress (IREC), IEEE, 2019, pp. 1–5, https://doi.org/10.1109/IREC.2019.8754516.

[11] A. Zeinalzadeh, A. Estebsari, A. Bahmanyar, Simultaneous optimal placement and sizing of DSTATCOM and parallel capacitors in distribution networks using multi-objective PSO, in: IEEE Milan PowerTech, IEEE, 2019, pp. 1–6, https://doi.org/10.1109/PTC.2019.8810577, 2019.

[12] M. Asadi, et al., Optimal placement and sizing of capacitor banks in harmonic polluted distribution network, in: 2021 IEEE Texas Power and Energy Conference (TPEC), IEEE, 2021, pp. 1–6, https://doi.org/10.1109/TPEC51183.2021.9384992.

[13] G. Boone, H.-D. Chiang, Optimal capacitor placement in distribution systems by genetic algorithm, Int. J. Electr. Power Energy Syst. 15 (3) (1993) 155–161, https://doi.org/10.1016/0142-0615(93)90030-Q. .

[14] M. Šarić, J. Hivziefendić, Optimal capacitor placement in distribution network for loss reduction and voltage profile improvement, in: 2019 18th International Symposium INFOTEH-JAHORINA (INFOTEH), IEEE, 2019, pp. 1–4, https://doi.org/10.1109/INFOTEH.2019.8717769. .

[15] G. Carpinelli, P. Varilone, V. Di Vito, A. Abur, Capacitor placement in three-phase distribution systems with nonlinear and unbalanced loads, IEE Proc. Generat. Transm. Distrib. 152 (1) (2005) 47–52, https://doi.org/10.1049/ip-gtd:20040709.

[16] M.-R. Haghifam, O. Malik, Genetic algorithm-based approach for fixed and switchable capacitors placement in distribution systems with uncertainty and time varying loads, IET Gener., Transm. Distrib. 1 (2) (2007) 244–252, https://doi.org/10.1049/iet-gtd:20045267. .

[17] J. Grainger, S. Lee, Capacity release by shunt capacitor placement on distribution feeders: a new voltage-dependent model, IEEE Trans. Power Apparatus Syst. (5) (1982) 1236–1244, https://doi.org/10.1109/TPAS.1982.317385.

[18] B. Venkatesh, R. Ranjan, Fuzzy EP algorithm and dynamic data structure for optimal capacitor allocation in radial distribution systems, IEE Proc. Generat. Transm. Distrib. 153 (1) (2006) 80–88, https://doi.org/10.1049/ip-gtd:20050054.

[19] A. Arief, M.B. Nappu, An analytical method for optimal capacitors placement from the inversed reduced jacobian matrix, Energy Proc. 100 (2016) 307–310, https://doi.org/10.1016/j.egypro.2016.10.182.

[20] Y. Bae, Analytical method of capacitor allocation on distribution primary feeders, IEEE Trans. Power Apparatus Syst. (4) (1978) 1232–1238, https://doi.org/10.1109/TPAS.1978.354605.

[21] M. Sedighizadeh, R. Bakhtiary, Optimal multi-objective reconfiguration and capacitor placement of distribution systems with the Hybrid Big Bang–Big Crunch algorithm in the fuzzy framework, Ain Shams Eng. J. 7 (1) (2016) 113–129, https://doi.org/10.1016/j.asej.2015.11.018.

[22] A.Y. Abdelaziz, E.S. Ali, S.M. Abd Elazim, Flower pollination algorithm for optimal capacitor placement and sizing in distribution systems, Elec. Power Compon. Syst. 44 (5) (2016) 1–12, https://doi.org/10.1080/15325008.2015.1117540.

[23] T. Jayabarathi, T. Raghunathan, R. Sanjay, A. Jha, S. Mirjalili, S.H.C. Cherukuri, Hybrid grey wolf optimizer based optimal capacitor placement in radial distribution systems, Elec. Power Compon. Syst. (2022) 1, https://doi.org/10.1080/15325008.2022.2132556. –13.

[24] M.H.M. Jahromi, P. Dehghanian, M.R.M. Khademi, M.Z. Jahromi, Reactive power compensation and power loss reduction using optimal capacitor placement, in: 2021 IEEE Texas Power and Energy Conference (TPEC), IEEE, 2021, pp. 1–6, https://doi.org/10.1109/TPEC51183.2021.9384963.

[25] A. Konak, D.W. Coit, A.E. Smith, Multi-objective optimization using genetic algorithms: a tutorial, Reliab. Eng. Syst. Saf. 91 (9) (2006) 992–1007, https://doi.org/10.1016/j.ress.2005.11.018. .

[26] M. Abd-Elhameed, A.A. El-Fergany, Water cycle algorithm-based economic dispatcher for sequential and simultaneous objectives including practical constraints, Appl. Soft Comput. 58 (2017) 145–154, https://doi.org/10.1016/j.asoc.2017.04.046.

[27] L. Belhoul, L. Galand, D. Vanderpooten, An efficient procedure for finding best compromise solutions to the multi-objective assignment problem, Comput. Oper. Res. 49 (2014) 97–106, https://doi.org/10.1016/j.cor.2014.03.016.

[28] B.-J. Liu, X.-J. Bi, Adaptive ε-constraint multi-objective evolutionary algorithm based on decomposition and differential evolution, IEEE Access 9 (2021) 17596–17609, https://doi.org/10.1109/ACCESS.2021.3053041. .

[29] I. Aljarah, et al., A robust multi-objective feature selection model based on local neighborhood multi-verse optimization, IEEE Access 9 (2021) 100009–100028.

[30] Z. Zhao, et al., An adaptive multi-objective salp swarm algorithm for efficient demand side management, in: 2020 IEEE 17th International Conference on Mobile Ad Hoc and Sensor Systems (MASS), IEEE, 2020, pp. 292–299, https://doi.org/10.1109/MASS50613.2020.00044. .

[31] M. Bajaj, N.K. Sharma, M. Pushkarna, H. Malik, M.A. Alotaibi, A. Almutairi, Optimal design of passive power filter using multi-objective pareto-based firefly algorithm and analysis under background and load-side's nonlinearity, IEEE Access 9 (2021) 22724–22744, https://doi.org/10.1109/ACCESS.2021.3055774.

[32] Z.A.A. Alyasseri, A.T. Khader, M.A. Al-Betar, J.P. Papa, O.A. Alomari, EEG feature extraction for person identification using wavelet decomposition and multi-objective flower pollination algorithm, IEEE Access 6 (2018) 76007–76024, https://doi.org/10.1109/ACCESS.2018.2881470.

[33] A. Pajares, X. Blasco, J.M. Herrero, G. Reynoso-Meza, A new point of view in multivariable controller tuning under multiobjective optimization by considering nearly optimal solutions, IEEE Access 7 (2019) 66435–66452, https://doi.org/10.1109/ACCESS.2019.2915556.

[34] H. Kargaran, S. Yazdani, Set of Pareto solutions for optimum cascade problems using MOPSO algorithm, Res. Eng. 16 (2022) 1–9, https://doi.org/10.1016/j.rineng.2022.100625.

[35] S.M. Tabatabaei, B. Vahidi, Bacterial foraging solution based fuzzy logic decision for optimal capacitor allocation in radial distribution system, Elec. Power Syst. Res. 81 (4) (2011) 1045–1050, https://doi.org/10.1016/j.epsr.2010.12.002.

[36] T. Huang, Y. Hsiao, C. Chang, J. Jiang, Optimal placement of capacitors in distribution systems using an immune multi-objective algorithm, Int. J. Electr. Power Energy Syst. 30 (3) (2008) 184–192, https://doi.org/10.1016/j.ijepes.2007.06.012.

[37] A. Rajendran, K. Narayanan, Multi-objective hybrid WIPSO–GSA algorithm-based DG and capacitor planning for reduction of power loss and voltage deviation in distribution system, Smart Sci. 6 (4) (2018) 1–13, https://doi.org/10.1080/23080477.2018.1488206.

[38] S.M.S. Danish, M. Ahmadi, A. Yona, T. Senjyu, N. Krishna, H. Takahashi, Multi-objective optimization of optimal capacitor allocation in radial distribution systems, Int. J. Emerg. Elec. Power Syst. 21 (3) (2020) 1–11, https://doi.org/10.1515/ijeeps-2019-0206.

[39] K. Deb, Multi-objective optimisation using evolutionary algorithms: an introduction, in: Multi-objective Evolutionary Optimisation for Product Design and Manufacturing, Springer, 2011.

[40] K. Deb, A. Pratap, S. Agarwal, T. Meyarivan, A fast and elitist multiobjective genetic algorithm: NSGA-II, IEEE Trans. Evol. Comput. 6 (2) (2002) 182–197, https://doi.org/10.1109/4235.996017.
[41] S. Panda, Multi-objective PID controller tuning for a FACTS-based damping stabilizer using non-dominated sorting genetic algorithm-II, Int. J. Electr. Power Energy Syst. 33 (7) (2011) 1296–1308, https://doi.org/10.1016/j.ijepes.2011.06.002. .
[42] S. Mirjalili, S. Saremi, S.M. Mirjalili, L.D.S. Coelho, Multi-objective grey wolf optimizer: a novel algorithm for multi-criterion optimization, Expert Syst. Appl. 47 (2016) 106–119, https://doi.org/10.1016/j.eswa.2015.10.039.
[43] A. El-Fergany, Multi-objective allocation of multi-type distributed generators along distribution networks using backtracking search algorithm and fuzzy expert rules, Electr, Power Compon. Syst. 44 (3) (2016) 252–267, https://doi.org/10.1080/15325008.2015.1102989.
[44] S.K. Injeti, V.K. Thunuguntla, M. Shareef, Optimal allocation of capacitor banks in radial distribution systems for minimization of real power loss and maximization of network savings using bio-inspired optimization algorithms, Int. J. Electr. Power Energy Syst. 69 (2015) 441–455, https://doi.org/10.1016/j.ijepes.2015.01.040. .
[45] A.A. El-Fergany, A.Y. Abdelaziz, Capacitor placement for net saving maximization and system stability enhancement in distribution networks using artificial bee colony-based approach, Int. J. Electr. Power Energy Syst. 54 (2014) 235–243, https://doi.org/10.1016/j.ijepes.2013.07.015.
[46] A.R. Abul'Wafa, Optimal capacitor placement for enhancing voltage stability in distribution systems using analytical algorithm and Fuzzy-Real Coded GA, Int. J. Electr. Power Energy Syst. 55 (2014) 246–252, https://doi.org/10.1016/j.ijepes.2013.09.014. .
[47] M. Chakravorty, D. Das, Voltage stability analysis of radial distribution networks, Int. J. Electr. Power Energy Syst. 23 (2) (2001) 129–135, https://doi.org/10.1016/S0142-0615(00)00040-5. .
[48] D.S. Rani, N. Subrahmanyam, M. Sydulu, Self adaptive harmony search algorithm for optimal capacitor placement on radial distribution systems, in: International Conference on Energy Efficient Technologies for Sustainability, IEEE, 2013, pp. 1330–1335, https://doi.org/10.1109/ICEETS.2013.6533580, 2013.
[49] C.-C. Lee, Fuzzy logic in control systems: fuzzy logic controller. I, IEEE Trans. Syst., Man, Cybern. 20 (2) (1990) 404–418, https://doi.org/10.1109/21.52552.
[50] S. Panda, N.K. Yegireddy, Automatic generation control of multi-area power system using multi-objective non-dominated sorting genetic algorithm-II, Int. J. Electr. Power Energy Syst. 53 (2013) 54–63, https://doi.org/10.1016/j.ijepes.2013.04.003.
[51] J. Hazra, A. Sinha, A multi-objective optimal power flow using particle swarm optimization, Eur. Trans. Electr. Power 21 (1) (2011) 1028–1045, https://doi.org/10.1002/etep.494.
[52] T. Gözel, M.H. Hocaoglu, An analytical method for the sizing and siting of distributed generators in radial systems, Electr, Power Syst. Res. 79 (6) (2009) 912–918, https://doi.org/10.1016/j.epsr.2008.12.007.
[53] M.E. Baran, F.F. Wu, Network reconfiguration in distribution systems for loss reduction and load balancing, IEEE Trans. Power Deliv. 4 (2) (1989) 1401–1407, https://doi.org/10.1109/61.25627. .
[54] Y.M. Shuaib, M.S. Kalavathi, C.C.A. Rajan, Optimal capacitor placement in radial distribution system using gravitational search algorithm, Int. J. Electr. Power Energy Syst. 64 (2015) 384–397, https://doi.org/10.1016/j.ijepes.2014.07.041.
[55] D.F. Pires, C.H. Antunes, A.G. Martins, An NSGA-II Approach with Local Search for a VAR Planning Multi-Objective Problem, 2009.